Materials Characterization 118 (2016) 225–234

Contents lists available at ScienceDirect

Materials Characterization

journal homepage: www.elsevier.com/locate/matchar

Characterization of as-welded microstructure of heat-affected zone in modified 9Cr–1Mo–V–Nb steel weldment

Yiyu Wang, Rangasayee Kannan, Leijun Li *

Department of Chemical and Materials Engineering, University of Alberta, Edmonton, Alberta, T6G 2V4, Canada

ARTICLE INFO

Article history:
Received 6 April 2016
Received in revised form 26 May 2016
Accepted 28 May 2016
Available online 29 May 2016

Keywords:
P91 weldment
Microstructure
Heat-affected zone
EBSD

ABSTRACT

Non-equilibrium microstructure of the heat-affected zone (HAZ) in the as-welded modified 9Cr–1Mo–V–Nb pipe steel (P91) weldment deposited by gas tungsten arc welding (GTAW) and flux core arc welding (FCAW) has been characterized by field-emission scanning electron microscope (FESEM) and electron backscatter diffraction (EBSD). The heterogeneous structures in the sub-layers of the as-welded HAZ are attributable to phase transformations caused by the welding thermal cycles and the local structure variations in the as-received base metal. Coarse-grained heat-affected zone (CGHAZ) has a prior austenite grain (PAG) size of 20 μm. Fine uniformly-distributed precipitates and a higher fraction of MX carbonitrides are observed in the CGHAZ. Fine-grained heat-affected zone (FGHAZ) consists of the finest grains (1.22 μm measured by EBSD, 5 μm PAG size), coarse undissolved $M_{23}C_6$ carbides within the PAG boundaries and fine nucleated $M_{23}C_6$ particles within the martensite laths. Intercritical heat-affected zone (ICHAZ) consists of partially austenitized grains and over-tempered martensite laths. EBSD kernel average misorientation (KAM) map in the FGHAZ close to the ICHAZ illustrates the greatest local strain variations with a moderate normalized KAM value of 0.92°. The majority (88.1%) of the matrix grains in the CGHAZ are classified as deformed grains by EBSD grain average misorientation (GAM) evaluation. The FGHAZ close to the ICHAZ has the most recrystallized grains with an area fraction of 14.4%. The highest density variation of precipitates within grains in the FGHAZ originates from the inhomogeneous chemistry in the base metal.

1. Introduction

Modified 9Cr–1Mo–V–Nb pipe steel (P91) is a creep-enhanced martensitic-ferritic steel that is widely used in the fossil fired power plants [1–4]. Fusion welding processes, such as gas tungsten arc welding (GTAW), flux core arc welding (FCAW), and submerged arc welding (SAW), are commonly used to weld P91 steel [5–8]. However, the structure of tempered martensite with finely dispersed $M_{23}C_6$ and MX of the as-received P91 steel is susceptible to drastic changes during fusion welding thermal cycle. A narrow non-equilibrium heat-affected zone (HAZ) in the base metal of the weldment is generated after the welding thermal cycle. The HAZ experiences on-heating peak temperatures ranging from just above A_{c1} to close to the melting temperature T_m, and cools down to room temperature within a few minutes. Sub-layers exist within the entire HAZ are divided into coarse-grained heat-affected zone (CGHAZ), fine-grained heat-affected zone (FGHAZ), and intercritical heat-affect zone (ICHAZ) according to the peak temperatures [9,10]. Fig. 1 shows a schematic fusion welding peak temperature profile and the typical microstructure in various heat-affected zones of the as-welded P91 steel weldment. Due to the high heating and cooling rates, a few phase transformations occur in the HAZ, including diffusive austenitic phase transformation on-heating, diffusionless martensitic transformation on-cooling, and precipitate dissolution or coarsening during the thermal cycle.

Microstructure of the HAZ in P91 welds, including size, shape, and distribution of grains and precipitates, is critical to keeping their long-term creep resistance during their service under high temperature and pressure. The infamous Type IV creep rupture that often occurs in the FGHAZ or ICHAZ is a challenging issue for P91 steel applications [11–13]. P91 weldments are normally post-weld heat treated (PWHT) to optimize the structure and to reduce the residual stresses after welding and before being put into high temperature service. After PWHT, the matrix grain growth and coarsening of $M_{23}C_6$ carbides are observed in the FGHAZ and ICHAZ, which leads to lower hardness values in FGHAZ and ICHAZ. As a complex structural evolution happens after the PWHT into the creep service, the seemingly disappeared FGHAZ becomes the primary location for the Type IV failure of the heat-treated P91 weldments at the FGHAZ close to ICHAZ. Many studies have investigated the microstructure of P91 HAZ after PWHT [14,15]. It is notable that only few studies focused on the as-welded HAZ microstructure, Sawada et al. [16] was one of those who investigated the various distributions of

* Corresponding author.
E-mail address: leijun@ualberta.ca (L. Li).

http://dx.doi.org/10.1016/j.matchar.2016.05.024
1044-5803/

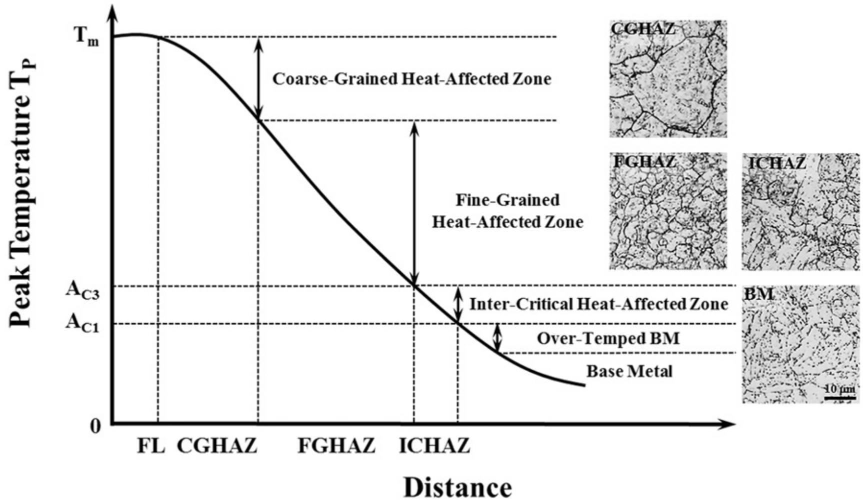

Fig. 1. A schematic fusion welding peak temperature profile and the typical microstructure in the heat-affected zone (HAZ) of the as-welded P91 steel weldment.

Table 1
Chemical composition of Grade 91 base metal (P91) and filler metals used in this study (wt%).

Materials	C	Cr	Mo	Mn	Si	Ni	Al	V	Nb	S	P	N
ER90S-B9 GTAW	0.097	8.830	0.928	0.560	0.250	0.307	0.002	0.197	0.064	0.004	0.006	0.030
E91T1-B9 FCAW	0.100	8.830	0.880	0.790	0.280	0.550	0.001	0.200	0.030	0.008	0.020	0.050
Base metal	0.110	8.470	0.940	0.370	0.370	0.080	0.002	0.190	0.071	0.002	0.016	0.048

$M_{23}C_6$ and MX particles along the cross-sectional modified 9Cr–1Mo weld in as-welded condition. The as-welded microstructure has been largely ignored in many reports, possibly because P91 requires a PWHT before being put into service. Yet the initial structure in the HAZ immediately after welding may be directly responsible for the subsequent structural evolution during the PWHT as well as in the high temperature creep service.

With the availability of electron backscatter diffraction (EBSD) technique, new and quantitative analyses of grain orientation and phase distribution of crystalline materials can be applied to the welded joints [17–19]. Recent EBSD works on the structure evolution of matrix grains in P91 base metal have been reported [20–22], but characterization of the sub-layers in the as-welded HAZ has not been reported systematically. Furthermore, EBSD characterization of the precipitates in the HAZ has not been reported due to their small size and EBSD analysis depth. In addition, due to the strength mismatch between the dispersive precipitates and matrix grains, local strain levels are variable at different locations of a grain and across grain boundaries. Visualization of this local strain distribution is difficult for other traditional methods, such as TEM and XRD, but becomes possible by using the EBSD technique. The purpose of this work is to characterize the non-equilibrium substructures of the HAZ in P91 weldments right after the welding thermal cycle by field-emission SEM (FESEM) and EBSD. Matrix microstructure variation and precipitate distribution in the as-welded HAZ are investigated systematically for the first time to provide more understanding of Type IV creep rupture mechanism of the P91 weldments.

2. Materials and experimental procedure

P91 steel was used as the base metal in this work. The as-received pipe has a 219 mm (8.625 in) outer diameter (OD) and 29 mm (1.143 in) thickness. It was normalized for 8 min at 1060 °C and tempered for 45 min at 786 °C. Flux cored arc welding (FCAW) and gas tungsten arc welding (GTAW) were used to weld two 124 mm long pipes with a 60° double-V weld groove and 1.5 mm root face, respectively. Chemical compositions of P91 base metal, GTAW filler metal ER90S-B9 (1.2 mm diameter) and FCAW filler metal ER91T1-B9 (1.2 mm diameter) are presented in Table 1. GTAW parameters used for the root pass were 300 A DC and 1.27 m/min wire feed speed. FCAW parameters for the filling passes were 26.1 and 27 arc voltage and 6.35 and 7.62 m/min wire feed speed. A stepper motor controlled fixture was used to maintain 0.14 m/min linear travel speed. A preheat temperature of 150 °C, an interpass temperature of 300 °C, and a wire feed speed of 7620 mm/min at 27 V were selected. Shielding gases used for GTAW and FCAW were pure argon and mixed 75/25 argon/CO_2, respectively. For hydrogen bake-out, a post-weld isothermal hold was conducted at 250 °C for 4 h.

Vickers hardness across the cross-section of polished welds was measured with 0.5 kgf and a dwell time of 10 s by using Tukon 2500 automated hardness tester. For microstructure characterization, cross-sectional specimens were cut from the as-weld P91 weld. These specimens were mounted, grinded and polished by using a controlled mechanical polishing method. Grit #360, #600, #1200 SiC sand papers were used for grinding. 3 μm and 1 μm diamond suspension, 0.5 μm and 0.05 μm alumina suspension and 0.02 μm colloidal silica were used for polishing.

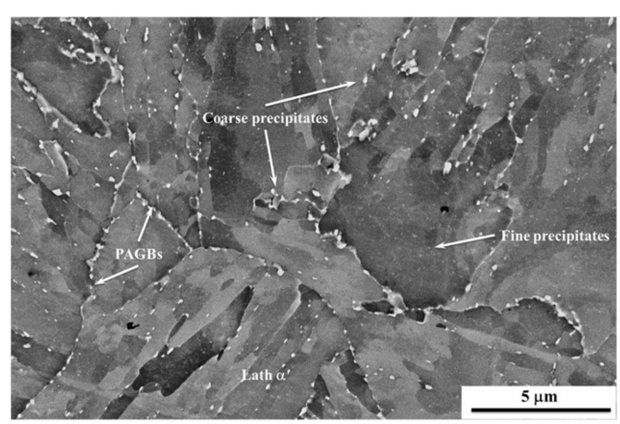

Fig. 2. Typical microstructure of the as-received P91 base metal (backscattered electron image).